

Efficient Inference Using Large Language Models with Limited Human Data: Fine-Tuning then Rectification

Lei Wang

Foster School of Business, University of Washington, Seattle, WA, lei0603@uw.edu

Zikun Ye

Foster School of Business, University of Washington, Seattle, WA, zikunye@uw.edu

Jinglong Zhao

Questrom School of Business, Boston University, Boston, MA, jinglong@bu.edu

Driven by recent advances in artificial intelligence (AI), a growing body of work demonstrates the potential of using large language models (LLMs) to generate human-like responses in market research and social science applications. Two primary approaches can be applied to improve the performance of LLMs: fine-tuning, which aligns LLM predictions more closely with human responses, and rectification, which corrects biases in LLM outputs. In this paper, we develop a framework that combines fine-tuning and rectification, and optimally allocates limited labeled samples across the two stages. Unlike the conventional objective that minimizes the mean squared prediction errors, we propose to minimize the variance of the prediction errors as the fine-tuning objective, which is optimal for the downstream rectification stage. Building on this insight, we leverage empirical scaling laws to develop a data-driven method for optimally splitting samples between the fine-tuning and rectification stages. Empirical analysis validates our framework, demonstrating improved estimation and inference performance compared to using either fine-tuning or rectification alone.

Key words: Large Language Models, Fine-Tuning, Prediction-Powered Inference

History: This version: November 26, 2025

1. Introduction

The rapid development of artificial intelligence (AI) technologies, especially large language models (LLMs), has demonstrated the potentials of using large language models as human surrogates in survey-based research across disciplines, including economics, social science, and marketing. Traditional survey-based research is often costly, time-consuming, and difficult to scale. By contrast, LLMs offer the possibility of simulating human responses at near-zero marginal cost, motivating growing interests in using LLMs as surrogates for human respondents in a wide range of business applications.

LLMs are trained on massive corpora of human-generated text, enabling them to internalize patterns of preferences, beliefs, and behavior. Recent studies demonstrate that LLMs can closely approximate human responses in many market research and social science tasks (Brand et al. 2023, Li et al. 2024, Liu et al. 2024, Toubia et al. 2025). This positions LLMs as a potentially

powerful surrogate for human participants. For academic researchers, LLM-based respondents can substantially reduce the time and cost associated with pilot testing and survey design. For industry practitioners, the ability to rapidly screen ideas, test product concepts, or forecast consumer reactions offers clear operational and strategic advantages. As a result, LLM-as-proxy has become an increasingly attractive tool for accelerating insight generation in business contexts.

Despite this promise, using LLMs as substitutes for human respondents faces substantial challenges. Off-the-shelf LLMs are not optimized for producing accurate or human-aligned responses, as their pretraining objective is to predict the next token rather than to replicate human judgments or preferences. Empirical studies document consistent biases and systematic deviations between LLM outputs and human survey responses (Motoki et al. 2024, Li et al. 2025). LLM predictions are also highly sensitive to prompt formulations and model architectures, which can generate instability across seemingly minor design changes (Brucks and Toubia 2023). One can improve LLM response accuracy through techniques that operate during inference without updating model parameters, such as chain-of-thought prompting to elicit step-by-step reasoning (Wei et al. 2022), in-context learning with several demonstrations to clarify the task (Brown et al. 2020), and persona conditioning to emulate specific subpopulations (Peng et al. 2025). These approaches are appealing because they are model-agnostic and easy to deploy. However, their reliability in accurately reproducing human counterparts remains uncertain (Pezeshkpour and Hruschka 2024, Ye et al. 2025, Krsteski et al. 2025).

These limitations of prompting highlight the need for methodological advances that more effectively leverage LLMs as human surrogates. In practice, assessing whether an LLM is suitable for a specific task requires some labeled samples, which also enable us to improve or correct the model when its outputs deviate from human data. Broadly, existing approaches fall into two families. The first family updates model parameters during the post-training phase through fine-tuning on labeled task data. Essentially, fine-tuning aligns the conditional response distribution more closely with human data, improving the accuracy on domain-specific tasks and demonstrating success across many business applications (Angelopoulos et al. 2024, Ye et al. 2025, Cheng et al. 2025). Its computational cost has become increasingly manageable. For example, Parameter-efficient fine-tuning methods such as LoRA train only small low-rank adapters (Hu et al. 2022), and recent surveys find that PEFT techniques can approach the accuracy of full fine-tuning at a fraction of the cost (Han et al. 2024). The main limitation of fine-tuning is the requirement for scarce task-specific labeled data. Scaling laws further indicate diminishing returns as the size of the labeled dataset increases (Zhang et al. 2024). Moreover, it is often unclear how to assess the true marginal value of additional labeled samples for fine-tuning or how much bias remains in the LLM after fine-tuning.

The second family of methods focuses on post-hoc rectification without updating LLM parameters. These approaches treat the pretrained LLM as a powerful yet biased black-box predictor and correct its outputs using a small labeled sample. Prediction-Powered Inference (PPI) is a prominent example. PPI combines plentiful LLM predictions with an independent labeled dataset to construct unbiased estimators and valid confidence intervals (Angelopoulos et al. 2023a). Although PPI does not modify the LLM, it nonetheless, similar to fine-tuning, requires labeled data samples to correct model bias. Moreover, the variance of a PPI estimator decreases with additional labeled data but exhibits diminishing returns. Other post-hoc rectification methods also exist. For example, Wang et al. (2024) propose a transfer-learning-based correction for LLM bias. In this paper, we focus on the standard PPI framework for clarity, though our core insights extend to other post-hoc rectification approaches.

Importantly, PPI requires that the labeled data used for rectification be completely separate from any data used to train or fine-tune the predictive model, in order to preserve the independence guarantees essential for valid inference. Together, these observations motivate our central design question: *Can combining fine-tuning and post-hoc rectification yield better performance than either method alone, and if so, how should such a framework be designed?* In particular, given the limited human-labeled samples, how should one (adaptively) allocate samples between fine-tuning, which improves surrogate predictions, and PPI, which further debiases these predictions, to optimize downstream estimation and inference performance?

We address these questions by analyzing how the variance of the PPI estimator depends on the quality of the LLM’s predictions. This analysis allows us to identify the fine-tuning objective that is optimal for the subsequent PPI correction step, yielding the lowest possible PPI variance. Unlike conventional objectives that minimize average prediction error, our proposed objective minimizes the variability of the prediction errors, which is the quantity that governs PPI’s statistical efficiency. Building on this insight, we then develop a data-driven method for allocating labeled samples between fine-tuning and PPI, guided by empirical scaling laws of LLM. A large body of evidence shows that LLM performance improves in smooth, predictable ways as model size and data scale increase, often following simple power-law patterns in both pre-training and fine-tuning stages (Kaplan et al. 2020, Hernandez et al. 2021, Hoffmann et al. 2022). In our setting, these patterns describe how the quality of the fine-tuned predictor improves with additional labeled data, enabling us to characterize the optimal split of limited samples between improving the model and correcting its residual bias through PPI. To our knowledge, this is the first work to formally analyze the interaction between fine-tuning and PPI. A recent empirical study finds that combining the two methods can improve accuracy relative to using either one alone (Krsteski et al. 2025), but it relies on standard fine-tuning procedures that are not optimized for the downstream correction step. In

contrast, our framework derives the fine-tuning objective that is optimal for PPI and provides a principled approach to allocating labeled samples across the two stages.

We further conduct an empirical study on the EmoBank dataset, a 10k-sentence corpus annotated with continuous emotion scores, to evaluate our framework. The task is to estimate the population mean from limited labeled data ($n = 500$). In the fine-tuning stage, we replace the standard MSE objective with a variance-based loss, which is optimal for the downstream PPI. We have four major findings. First, we have empirically validated the scaling law in the LLM fine-tuning setting with a very strong fit ($R^2 = 0.848$), which further validates our proposed data-driven ramp-up method for finding the optimal allocation rule. Second, we evaluate the variance-based loss and observe that it yields predictions more compatible with PPI than those from standard objectives. Third, we test the theoretically derived optimal sample-allocation rule and demonstrate that the resulting allocation matches the empirically best-performing split of labeled data between fine-tuning and rectification. Finally, we show that combining fine-tuning with PPI achieves a more efficient use of limited labeled data than applying either method alone.

Our contributions are threefold. First, to the best of our knowledge, we are the first to systematically investigate the interaction between fine-tuning and post-hoc rectification when using LLMs as human surrogates under limited labeled data. Second, we develop a unified framework that introduces a new variance-based fine-tuning objective and a scaling-law-guided ramp-up procedure for optimally allocating labeled samples across the two stages. Third, we empirically validate our method using real data and demonstrate substantial improvements over using fine-tuning or rectification alone. We hope this work encourages further research on methods for leveraging LLMs in market research and social science applications, where reliable inference with scarce human data is increasingly important.

2. Related Literature

In this section, we review three strands of work that are most closely related to our framework.

LLM fine-tuning. Fine-tuning has become a standard and major approach to adapt pretrained language models to downstream tasks by updating model parameters using labeled samples (Brown et al. 2020, Ouyang et al. 2022). For large models, parameter-efficient fine-tuning methods, such as LoRA (Hu et al. 2022) introduce task-specific low-rank matrix adapters while freezing most parameters, making fine-tuning computationally efficient in practice. A large empirical literature on neural scaling laws shows that model performance tends to follow smooth power-law relationships with model size, data size, and compute scale (Kaplan et al. 2020, Hernandez et al. 2021, Hoffmann et al. 2022), providing us with a parametric function to link between additional labeled data and predictive quality. Other fine-tuning methods, such as RLHF and DPO, update models using a

separate trained reward model or preference data (Ouyang et al. 2022, Rafailov et al. 2023). Beyond vanilla fine-tuning with commonly used objective functions such as mean-squared and cross-entropy losses, recent work has started to modify objectives to target downstream estimands directly. For example, Vafa et al. (2025) propose a debiasing fine-tuning method for foundation models and then estimate the wage gap. In our proposed framework, we focus on the setting where the LLM is used as a surrogate within a PPI estimator and design a fine-tuning objective that directly minimizes the variance governing the efficiency of final estimators.

Prediction-powered inference (PPI). PPI method combines a small set of labeled samples with a large set of model predictions to construct unbiased estimators and confidence intervals for population-level estimands while treating the prediction model as a potentially biased black box (Angelopoulos et al. 2023a). Follow-up work develops more efficient variants, such as PPI++ (Angelopoulos et al. 2023b). Recent research further connects PPI to the classical surrogate-outcome literature, showing that PPI-type estimators can be interpreted as using predictions as surrogates and proposing recalibrated procedures that achieve improved efficiency (Ji et al. 2025). Our work builds on this line of research by taking the prediction model to be an LLM that can itself be improved via fine-tuning, and by explicitly designing both the fine-tuning objective and the allocation of labeled data so as to minimize the asymptotic variance of the PPI estimator.

LLMs for market research and social science. A growing body of research evaluates whether LLMs can serve as substitutes or complements to human respondents in market research and related social-science applications. In marketing and consumer research, Brand et al. (2023) examine the use of GPT to estimate willingness to pay, documenting mixed results: LLMs can reproduce aggregate patterns reasonably well, but they generate insufficient heterogeneity across individuals even after fine-tuning, and fine-tuned models struggle to extrapolate beyond the training distribution. Other work studies whether LLMs can reproduce human preferences or attitudes in specific domains, including intertemporal choice (Goli and Singh 2024) and brand perception (Li et al. 2024). In political science and computational social science, Argyle et al. (2023) propose using LLMs as proxies for human subpopulations, and Ziems et al. (2024) survey the emerging use of LLMs in computational social-science workflows, highlighting their potential to augment, rather than replace, human data. At the same time, several recent papers underscore important limitations. Gui and Toubia (2023) raise identification concerns when using LLMs to simulate human behavior from a causal-inference perspective, while Wang et al. (2024) show that LLM-generated responses are useful for data augmentation but may still exhibit systematic biases relative to human samples. Our contribution is methodological and complements this literature: rather than assessing LLMs as stand-alone survey respondents, we study how to combine fine-tuning and post-hoc debiasing (via PPI) when LLM outputs are used as surrogate responses, and how to allocate scarce

human-labeled data between improving the surrogate model and correcting its residual biases to obtain reliable population estimates.

3. Problem Setup

We consider a mean estimation problem in a semi-supervised learning setting where we have access to both a small, labeled dataset and a large, unlabeled dataset. Let there be n samples in the small labeled dataset $\mathcal{N} = \{(\mathbf{X}_i, Y_i)\}_{i=1}^n$, where each sample (\mathbf{X}_i, Y_i) is an independent and identically distributed (i.i.d.) replica of a representative random variable (\mathbf{X}, Y) sampled from a joint distribution $(\mathbf{X}, Y) \sim \mathcal{F}$. Let there be m samples in the large unlabeled dataset $\mathcal{M} = \{\tilde{\mathbf{X}}_j\}_{j=1}^m$, where each sample $\tilde{\mathbf{X}}_j$ is an i.i.d. replica of a representative random variable \mathbf{X} sampled from the marginal distribution $\mathbf{X} \sim \mathcal{F}_{\mathbf{X}}$, where $\mathcal{F}_{\mathbf{X}}$ stands for the marginal distribution over \mathbf{X} according to the joint distribution \mathcal{F} . Let $\mathcal{X} \times \mathcal{Y}$ be the set that \mathcal{F} takes values from. We also have access to a machine learning predictor $f: \mathcal{X} \rightarrow \mathcal{Y}$ that is trained on data independent of both datasets.

Given these two datasets and the predictor, as discussed earlier, there are two families of techniques for more effectively leveraging LLMs as human surrogates: fine-tuning, which adapts the model using labeled data, and post-hoc rectification, which corrects model predictions without modifying the model itself.

1. **Fine-Tuning (FT).** We can use the small labeled dataset to fine-tune the machine learning predictor, and use the fine-tuned machine learning predictor to make mean estimation.
2. **Prediction-Powered Inference (PPI).** We can use the small labeled dataset to measure the error of the machine learning predictor, and then rectify the errors on the large unlabeled dataset.

In this paper, we proposed to combine fine-tuning and prediction-powered inference to achieve the merits of both approaches. As each sample in the small labeled dataset can only be used either in fine-tuning (FT) or in prediction-powered inference (PPI), we study the optimal sample allocation of the n samples to FT and PPI.

For any $0 < s < n$, let s be the number of samples we allocate to FT. Consequently, $n - s$ is the number of samples we allocate to PPI. Let $f^{(s)}: \mathcal{X} \rightarrow \mathcal{Y}$ be the machine learning predictor that is fine-tuned on s samples of the small labeled dataset. We propose to use the prediction-powered estimator based on the fine-tuned predictor $f^{(s)}(\cdot)$, defined as follows,

$$\hat{\mu} = \frac{1}{n-s} \sum_{i=1}^{n-s} (Y_i - f^{(s)}(\mathbf{X}_i)) + \frac{1}{m} \sum_{j=1}^m f^{(s)}(\tilde{\mathbf{X}}_j). \quad (1)$$

It is easy to see that $\hat{\mu}$ as defined in (1) is unbiased,

$$\hat{\mu} = \mathbb{E}[Y] - \mathbb{E}[f^{(s)}(\mathbf{X})] + \mathbb{E}[f^{(s)}(\mathbf{X})] = \mathbb{E}[Y],$$

where the first equality is because \mathbf{X} from the small labeled dataset and from the large unlabeled dataset are sampled from the same distribution. As the estimator $\hat{\mu}$ is unbiased, the remainder of this paper will focus on minimizing its variance. Given the unbiased estimator, the remaining determinant of statistical accuracy is its variance. In other words, the mean-squared error of the estimator reduces to its variance, so lower variance directly implies more accurate estimates, narrower confidence intervals, and more efficient use of scarce labeled data. In the following, our goal is to combine fine-tuning and PPI to make the most effective use of limited human labels.

4. Our Method

In this section, we begin by analyzing the variance of the PPI estimator and derive its implications for how the LLM should be fine-tuned in Section 4.1. We then use the scaling law in fine-tuning to characterize the optimal allocation of labeled samples between fine-tuning and PPI in Section 4.2, assuming the exact fine-tuning scaling law is known. Finally, Section 4.3 introduces a data-driven ramp-up procedure for estimating the parameters of the parametric scaling law, which then informs the sample allocation rule and allows valid inference.

4.1. A New Loss Function in Fine-Tuning

We start by examining the variance of $\hat{\mu}$ as defined in (1), following the same analysis in [Angelopoulos et al. \(2023a\)](#).

$$\begin{aligned}
& \mathbb{E}[(\hat{\mu} - \mathbb{E}[Y])^2] \\
&= \mathbb{E}\left[\left(\frac{1}{n-s} \sum_{i=1}^{n-s} (Y_i - f^{(s)}(\mathbf{X}_i)) + \frac{1}{m} \sum_{j=1}^m f^{(s)}(\tilde{\mathbf{X}}_j) - \mathbb{E}[Y]\right)^2\right] \\
&= \mathbb{E}\left[\left(\frac{1}{n-s} \sum_{i=1}^{n-s} (Y_i - f^{(s)}(\mathbf{X}_i) + \mathbb{E}[f^{(s)}(\mathbf{X})] - \mathbb{E}[Y]) + \frac{1}{m} \sum_{j=1}^m (f^{(s)}(\tilde{\mathbf{X}}_j) - \mathbb{E}[f^{(s)}(\mathbf{X})])\right)^2\right] \\
&= \frac{1}{n-s} \sum_{i=1}^{n-s} \mathbb{E}\left[(Y_i - f^{(s)}(\mathbf{X}_i) + \mathbb{E}[f^{(s)}(\mathbf{X})] - \mathbb{E}[Y])^2\right] + \frac{1}{m} \sum_{j=1}^m \mathbb{E}\left[(f^{(s)}(\tilde{\mathbf{X}}_j) - \mathbb{E}[f^{(s)}(\mathbf{X})])^2\right] \\
&= \frac{1}{n-s} \text{Var}\left(Y - f^{(s)}(\mathbf{X})\right) + \frac{1}{m} \text{Var}\left(f^{(s)}(\mathbf{X})\right)
\end{aligned} \tag{2}$$

where the third equality is because $(Y_i - f^{(s)}(\mathbf{X}_i))$ and $f^{(s)}(\tilde{\mathbf{X}}_j)$ are independent.

Because we have a large unlabeled dataset, the second term is small when m is large. So we focus our attention primarily on the first term. We make the following two observations on the benefit of combining FT and PPI.

1. The first term in (2) decreases when $n - s$ increases. This observation indicates that the more data we use toward PPI, the smaller this term becomes.

2. The first term in (2) decreases when $\text{Var}(Y - f^{(s)}(\mathbf{X}))$ decreases. This observation indicates that the more data we use toward FT, the higher quality is the fine-tuned predictor $f^{(s)}(\cdot)$, which then makes $\text{Var}(Y - f^{(s)}(\mathbf{X}))$ smaller.

It is worth noting that the bias of the fine-tuned predictor $f^{(s)}(\cdot)$ does not play an important role in the expression in (2). Even when the fine-tuned predictor $f^{(s)}(\cdot)$ is biased, our estimator $\hat{\mu}$ as defined in (1) can still have a small variance, as long as the variance of $Y - f^{(s)}(\mathbf{X})$ is small. See Example 1 below.

EXAMPLE 1 (FINE-TUNING A BIASED PREDICTOR). We consider an extreme case where the fine-tuned predictor always under-predicts by a constant, that is, there exists $c > 0$ such that $Y - f^{(s)}(\mathbf{X}) = c$. In this case, the mean squared error $\text{E}[(Y - f^{(s)}(\mathbf{X}))^2] = c^2$ can be large. But the variance $\text{Var}(Y - f^{(s)}(\mathbf{X})) = 0$ is always equal to zero. This example suggests that we can totally use a biased predictor in our prediction-powered estimator. But the key is that the biased predictor should always produce a *constant* bias, as opposed to a *varying* bias.

Example 1 has an important implication. It implies that we should minimize the variance $\text{Var}(Y - f^{(s)}(\mathbf{X}))$ as the loss function in FT, which is different from the traditional use of mean squared error as the loss function.

4.2. Optimal Sample Allocation

Fine-tuning is a flexible method that allows us to use variance $\text{Var}(Y - f^{(s)}(\mathbf{X}))$ as the loss function. Empirically, it is widely accepted that fine-tuning can effectively reduce the loss of the LLM predictor following a smooth power-law relationship, i.e., scaling law (Kaplan et al. 2020, Hernandez et al. 2021, Hoffmann et al. 2022),

$$\text{Var}(Y - f^{(s)}(\mathbf{X})) = as^{-\alpha} + b,$$

where $\alpha, a, b > 0$ are positive constants.¹ These constants depend on both the task and the fine-tuning data.

When the constants are known, we can minimize variance in the expression in (2) by solving the following univariate optimization problem,

$$\min_{s \in (0, n)} \frac{\text{Var}(Y - f^{(s)}(\mathbf{X}))}{n - s} = \min_{s \in (0, n)} \frac{as^{-\alpha} + b}{n - s}. \quad (3)$$

We can express the optimal solution to (3) through the following theorem.

¹ Classical scaling-law formulations also incorporate model size as an independent variable. In our setting, we treat the underlying foundation model as fixed, because model-size choices are typically constrained by practical considerations such as privacy, available base models, and compatibility with downstream systems. Moreover, many open-weight foundation models offer only a small set of discrete size options—for example, OpenAI’s gpt-oss provides only 20B-parameter and 120B-parameter variants. Although model-size selection could be incorporated into our framework, we abstract away from this dimension and focus on allocating labeled data for fine-tuning and post-hoc correction.

THEOREM 1 (Optimal allocation). *The optimal solution to (3), s^* , is given as the unique solution to*

$$\alpha a n s^{-\alpha-1} - (\alpha + 1) a s^{-\alpha} - b = 0. \quad (4)$$

The optimal solution s^* can easily be calculated through numerically solving equation (4) through a binary search, using the property that the left-hand side of equation (4) is monotone decreasing in s .

4.3. A Ramp-up Procedure

So far we have discussed the optimal sample allocation when the constants in the scaling law are known. In this section, we propose a data-driven ramp-up procedure to estimate the constants in the scaling law.

We start with an overview of our procedure. We randomly partition the n samples of the small labeled dataset into three subsets: an FT subset, a validation subset, and a PPI subset. We use samples from the FT subset to fine-tune the machine learning predictor $f^{(s)}(\cdot)$. We use samples from the validation subset to estimate the parameters in the scaling law. We use samples from the PPI subset, together with the fine-tuned predictor $f^{(s)}(\cdot)$, to estimate $\hat{\mu}$.

Now we introduce some notation to rigorously define this procedure. Let the ramp-up procedure proceed in $k \geq 3$ stages. Let the sample size of the validation subset be n_v , which does not depend on k . We randomly draw n_v samples from the small unlabeled dataset \mathcal{N} to form \mathcal{N}_v , and fix this sample \mathcal{N}_v unchanged during the ramp-up procedure.

Recall that the ramp-up procedure proceeds in k stages. Let there be a k -grid of sample sizes $\{n_1, n_2, \dots, n_k\}$ such that $0 < n_1 < \dots < n_k < n$. We randomly draw a nested sequence of samples $\emptyset \subset \mathcal{N}_1 \subset \dots \subset \mathcal{N}_k \subset \mathcal{N}$ by first drawing n_k samples from the small unlabeled dataset \mathcal{N} to form \mathcal{N}_k , and then drawing n_{k-1} samples from \mathcal{N}_k to form \mathcal{N}_{k-1} , ..., and finally drawing n_1 samples from \mathcal{N}_2 to form \mathcal{N}_1 .

In stage $l \in [k]$, we fine-tune a predictor $f^{(n_l)}(\cdot)$ on sample \mathcal{N}_l . After obtaining the predictor $f^{(n_l)}(\cdot)$, we can use it to evaluate $\text{Var}(Y - f^{(n_l)}(\mathbf{X}))$ on the validation sample \mathcal{N}_v . Denote the following sample mean and sample variance estimators,

$$\begin{aligned} \hat{\theta}_{(1),l} &= \sum_{i \in \mathcal{N}_v} Y_i - f^{(n_l)}(\mathbf{X}_i), \\ \hat{\theta}_{(2),l} &= \sum_{i \in \mathcal{N}_v} (Y_i - f^{(n_l)}(\mathbf{X}_i) - \hat{\theta}_{(1),l})^2. \end{aligned}$$

After obtaining the sample variance estimator, we collect a pair of $(n_l, \hat{\theta}_{(2),l})$. We will then use all the pairs collected up to stage l , namely, $(n_1, \hat{\theta}_{(2),1}), \dots, (n_l, \hat{\theta}_{(2),l})$, to fit a scaling law,

$$(\hat{\alpha}, \hat{a}, \hat{b}) = \arg \min_{\alpha, a, b} \sum_{i=1}^l \left(\hat{\theta}_{(2),i} - a n_i^{-\alpha} - b \right)^2.$$

Finally, we can plug in the estimated parameters $(\hat{\alpha}, \hat{a}, \hat{b})$ to numerically solve equation (4). Suppose the solution to equation (4) is calculated as \hat{s}_l^* , and we will use \hat{s}_l^* to guide the ramp-up decision. If both $l < k$ and $\hat{s}_l^* > n_l$, we proceed with the ramp-up procedure, and go to stage $l + 1$. If either $l = k$ or $\hat{s}_l^* \leq n_l$, we stop by setting $s = n_l$. We then use all the remaining samples $\mathcal{N} \setminus (\mathcal{N}_v \cup \mathcal{N}_l)$ as the small labeled dataset to perform PPI and obtain the estimator $\hat{\mu}$.

5. Empirical Analysis

In this section, we present empirical evidence to validate our proposed framework. We examine four key components. First, we assess the goodness of fit of the fine-tuning scaling law and confirm that LLM performance improves with labeled data in a manner consistent with the assumed power-law structure. Second, we evaluate the benefits of using the variance-based loss function in fine-tuning and show that it yields predictors better aligned with the needs of PPI than traditional objectives. Third, we test the optimal sample-allocation rule and demonstrate that our theoretically derived allocation closely matches the empirically best-performing split of labeled data. Finally, we show that combining fine-tuning with PPI leads to more efficient use of limited labeled data than employing either method alone.²

5.1. Empirical Setup

Dataset. EmoBank is a 10k-sentence English dataset manually annotated with continuous Valence–Arousal–Dominance (VAD) scores from multiple human raters under both writer- and reader-perspective emotion interpretations (Buechel and Hahn 2017). The VAD framework is derived from the Pleasure–Arousal–Dominance (PAD) model of (Russell and Mehrabian 1977), which conceptualizes emotional responses along three psychological dimensions. Instead of discrete emotion labels, each text is annotated with numerical scores that quantify its emotional positivity (Valence), intensity (Arousal), and sense of control (Dominance). The sentences are collected from diverse sources such as blogs, news articles, fiction, and social media. In our experiments, we use only the Valence (V) dimension with the corresponding sentence text, for the one-dimensional target for evaluating our variance-based fine-tuning objective. Examples of dataset entries are in Table 1.

LLM Model Architecture. We treat a pretrained LLM as a sentence encoder and attach a lightweight regression head on top. Given an input text \mathbf{X} , we first tokenize it and feed it into **Qwen3-Embedding-0.6B**, obtaining the final hidden layer, denoted by $h(\mathbf{X}) \in \mathbb{R}^d$.

² In the next updated version of the paper, we will incorporate additional empirical analyses using human-labeled datasets across multiple domains. These datasets vary in size, task difficulty, and response types, allowing us to further assess the effectiveness and generalizability of our proposed method.

Table 1 Summary and example entries from the EmoBank dataset

Statistic	Value
Total samples	10,062
Valence mean / std	2.98 / 0.35
Text length mean / std	87.8 / 68.4
Example 1 (X)	“Remember what she said in my last letter?”
Valence (Y)	3.00
Example 2 (X)	“Goodwill helps people get off of public assistance.”
Valence (Y)	3.44

This embedding is then passed through a small MLP regression head, denoted by g_ψ , to get the final prediction,

$$\hat{y} = g_\psi(h(\mathbf{X})) \in \mathbb{R},$$

where g_ψ consists of two linear layers with a ReLU activation layer. We fine-tune the encoder LLM and MLP regression head jointly. Because we use a small LLM model, we use full parameter fine-tuning instead of LoRA.

Training Objective. Standard LLM fine-tuning typically minimizes a cross-entropy loss, which also means maximizing the conditional likelihood of the next token. In contrast, our goal is not the next token prediction but efficient PPI estimation and inference of a target estimand, so we adopt a variance-based regression objective as discussed in Section 4.1 and fine-tune the LLM model.

Specifically, at each epoch of the fine-tuning process, we can access a batch (say the batch size of k) of training examples from the labeled dataset $\mathcal{N} = \{(\mathbf{X}_i, Y_i)\}_{i=1}^n$, and the corresponding prediction $\hat{Y}_i = g_\psi(h_\phi(\mathbf{x}_i))$. We can compute residuals

$$r_i = Y_i - \hat{Y}_i, \quad i = 1, \dots, k,$$

and their batch mean

$$\bar{r} = \frac{1}{k} \sum_{i=1}^k r_i.$$

Our loss is the within-batch variance of the residuals:

$$\mathcal{L}_{\text{var}} = \frac{1}{k} \sum_{i=1}^k (r_i - \bar{r})^2. \quad (5)$$

Unlike mean-squared error, which jointly penalizes bias and variance, the variance loss in (5) focuses exclusively on reducing the conditional spread of the residuals. This separation is essential for the subsequent PPI correction, which removes remaining systematic bias using an independent labeled dataset, allowing the fine-tuning stage to specialize in variance reduction.

Given the above loss function, we then leverage the standard mini-batch stochastic gradient descent algorithm, AdamW, for fine-tuning. We use different learning rates for the base LLM model and the MLP head: smaller for the base LLM and larger for the regression head. We train with a batch size of $k = 32$ until convergence of the variance loss in (5).

5.2. Scaling-law Validation

Next, we present the scaling-law phenomenon in the EmoBank fine-tuning experiment. We first draw and fix 10,000 data points and then construct our fine-tuning subsets with varying sizes by repeatedly sampling from this dataset. After the training, the loss (variance) is then evaluated on the held-out validation set, which is the same for all experiments to ensure consistent evaluation.

The relationship between training dataset size and the loss (variance) on the validation set is shown in Figure 1b. The result shows that the validation variance decreases as the fine-tuning subset size increases.

To quantify how the variance-based objective decreases with the fine-tuning subset size s , we estimate the constants in the following parametric power-law form,

$$\text{Var}(Y - f^{(s)}(\mathbf{X})) = a s^{-\alpha} + b,$$

where a captures the initial variance level, α characterizes the decay rate, and b denotes the irreducible variance floor. Given heteroskedasticity across different subset sizes (each s is evaluated through 10 independent runs), we fit this model using variance-weighted nonlinear least squares. Specifically, each point is weighted by the inverse of its estimated sampling variance:

$$\hat{\alpha}, \hat{a}, \hat{b} = \arg \min_{\alpha, a, b} \sum_i \frac{(\text{Var}_i - (a s_i^{-\alpha} + b))^2}{\hat{\sigma}_i^2}.$$

where $\widehat{\text{Var}}_i = \hat{a} s_i^{-\hat{\alpha}} + \hat{b}$.

The empirical curve matches the scaling-law fit closely, showing that the variance-based objective follows a smooth and predictable scaling relationship. Performance improvements converge around $s \approx 500$, reflecting diminishing marginal gains as the training subset grows. The fitted parameters $a = 0.287$, $\alpha = 0.297$, and $b = 0.042$ describe the shape of this scaling curve. The value of a indicates that the validation variance starts from a high level when the SFT size is small. The estimate $\alpha = 0.297$ shows that variance decreases at a moderate but consistent rate. The relatively high goodness-of-fit value ($R^2 = 0.848$) indicates that this model explains most of the observed variation in the empirical curve. These results show that the variance-based objective scales effectively and can be reliably applied in the fine-tuning goal.

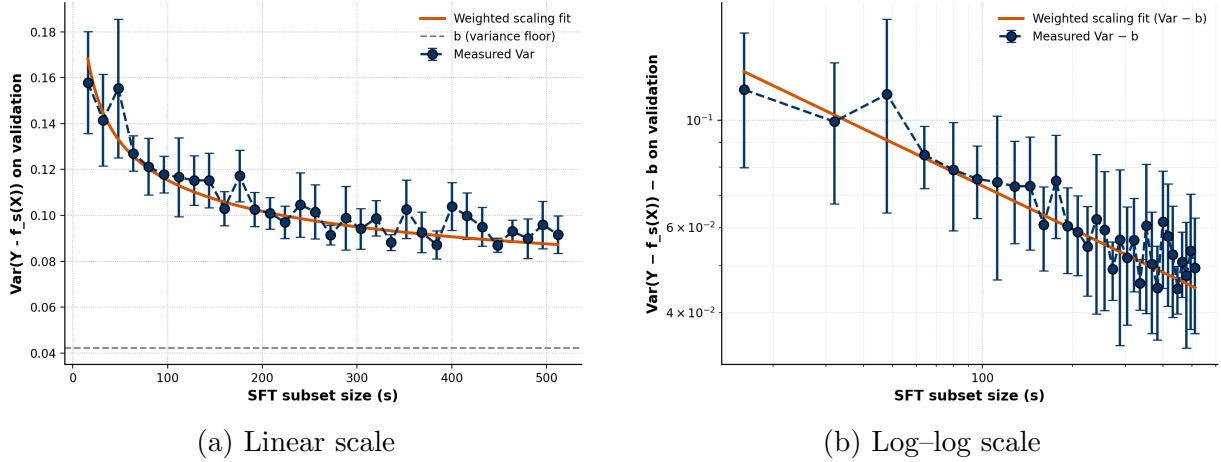


Figure 1 Scaling-law fit for the EmoBank dataset under linear and log-log scales with $\hat{\alpha} = 0.297$, $\hat{a} = 0.287$, $\hat{b} = 0.042$ and $R^2 = 0.848$.

Table 2 Comparison of estimation error (MAE) across four estimators

Labeled Data Size n	FT-Only	Sample Mean Estimator	PPI-Only	FT+PPI
$n = 500$	2.99	1.89×10^{-2}	3.75×10^{-2}	1.06×10^{-2}

Note: This table compares four estimators' errors. The sample mean estimator is defined as: $\hat{\mu}_{\text{sample mean}} = \sum_{i=1}^n Y_i / n$.

5.3. Comparison of Different Estimators

We compare the mean absolute error across four estimators assuming the total number of labeled samples is $n = 500$. From the result in Table 2, the key message is that our proposed method (FT+PPI) performs the best with the lowest MAE across four methods. Fine-tuning method performs the worst because it does not fully debias the error from the base LLM due to many factors, including but not limited to, approximation error, generalization error with limited training samples, and optimization error of neural network optimizers. One can observe that the sample-mean estimator works reasonably well. Although the sample mean estimator is unbiased, its variance can be large. The PPI-only estimator, although also unbiased, works worse than the sample mean estimator, mainly due to the large variance of the base LLM responses. Our proposed method to combine fine-tuning and PPI with optimally allocated samples works the best and achieves the lowest MAE across the methods, benefiting from a low-variance fine-tuned LLM and an unbiased correction term provided by the PPI rectification.

5.4. Optimal Allocation of Labeled Samples

After estimating the parameters in the scaling law of the form $a s^{-\alpha} + b$, we then apply Theorem 1 to compute the theoretically optimal allocation ratio based on these fitted parameters. Using these values, we get the theoretical optimal allocation for the EmoBank dataset, and compare it to other allocation ratios.

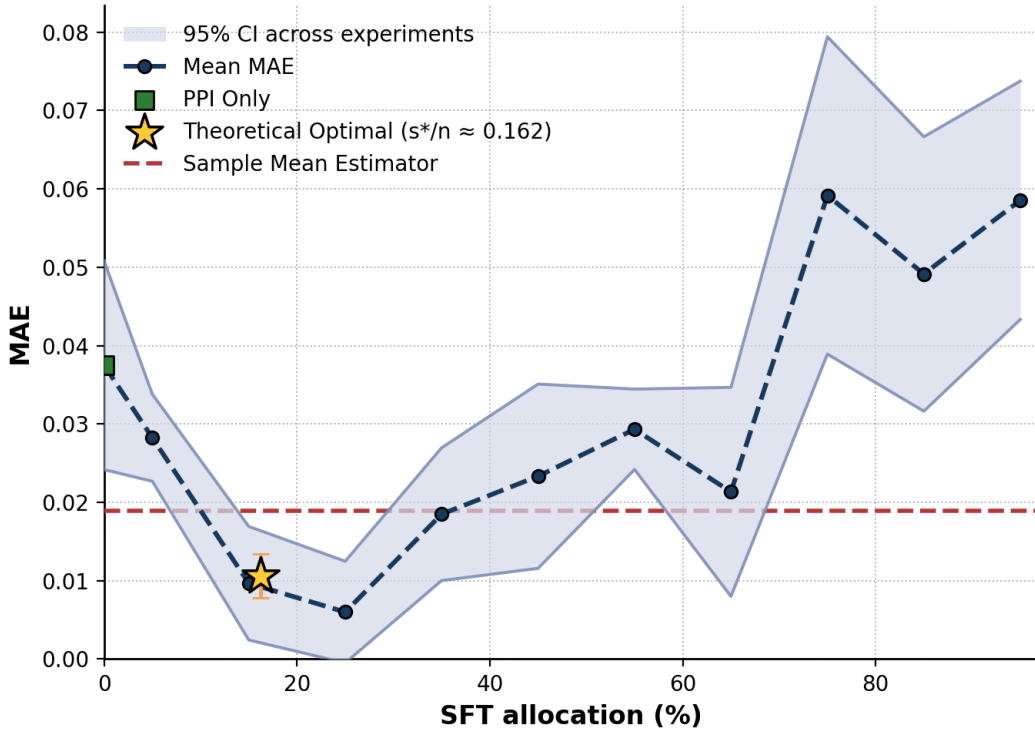


Figure 2 MAE performance of our proposed FT+PPI method under different labeled sample allocation ratios for FT. The total labeled sample size is $n = 500$.

The comparison result can be found in Figure 2, which displays the MAE as a function of the FT allocation percentage. It illustrates how the choice of FT/PPI split affects the estimator's accuracy with limited labeled samples.

First, this result basically confirms our variance decomposition of Equation (2) in Section 4.1, which shows the trade-off between FT and PPI regarding the variance reduction. Because the curve exhibits a clear U-Shaped pattern: with only a small portion of data samples for FT, the estimator suffers from high variance because the model is insufficiently fine-tuned and the resulting fine-tuned LLM still has high variance; In contrast, with too many data samples for FT, the remaining labeled data for PPI correction becomes too small, leading to increasing variance.

Another important observation is that the theoretical optimal allocation ratio (16.2%), as derived in Theorem 1, indeed aligns with the best empirical performance. In our numerical experiments, we vary the fine-tuning allocation using a 10% step size and evaluate ratios in $\{0\%, 5\%, 15\%, 25\%, \dots, 95\%\}$ for FT. Among these, the 25% allocation performs the best, but there is no statistically significant difference between 25% and the theoretical optimum of 16.2%. Taken together, these results confirm that our proposed FT+PPI approach, when paired with the optimal sample allocation, achieves the strongest overall empirical performance.

6. Conclusions

In this paper, we study how to more effectively leverage LLMs as human surrogates when only limited labeled data are available. We develop a unified framework that combines fine-tuning and post-hoc rectification and show that the variance of the PPI estimator provides a principled criterion for designing both the fine-tuning objective and the allocation of scarce labeled samples. Our analysis reveals that minimizing the variance of prediction errors—rather than the conventional mean-squared error—is optimal for downstream rectification. Building on this insight, we use empirical scaling laws to derive a data-driven rule for optimally splitting labeled samples between fine-tuning and rectification. Empirical evidence from the EmoBank dataset demonstrates that this integrated approach consistently outperforms either using fine-tuning or PPI alone, and that the theoretically optimal allocation closely aligns with the best-performing empirical split.

We view this work as an initial step toward a more systematic understanding of how to jointly use fine-tuning and rectification for efficient inference with limited human data. As LLMs become increasingly integrated into market research and social-science applications, developing principled methods for combining model improvement and statistical correction will be essential for generating reliable and trustworthy insights at scale.

References

Angelopoulos AN, Bates S, Fannjiang C, Jordan MI, Zrnic T (2023a) Prediction-powered inference. *Science* 382(6671):669–674.

Angelopoulos AN, Duchi JC, Zrnic T (2023b) PPI++: Efficient prediction-powered inference. *arXiv preprint arXiv:2311.01453* .

Angelopoulos P, Lee K, Misra S (2024) Causal alignment: Augmenting language models with a/b tests. *Available at SSRN 4781850* .

Argyle LP, Busby EC, Fulda N, Gubler JR, Rytting C, Wingate D (2023) Out of one, many: Using language models to simulate human samples. *Political Analysis* 31(3):337–351.

Brand J, Israeli A, Ngwe D (2023) Using llms for market research. *Harvard business school marketing unit working paper* (23-062).

Brown T, Mann B, Ryder N, Subbiah M, Kaplan JD, Dhariwal P, Neelakantan A, Shyam P, Sastry G, Askell A, et al. (2020) Language models are few-shot learners. *Advances in neural information processing systems* 33:1877–1901.

Brucks M, Toubia O (2023) Prompt architecture can induce methodological artifacts in large language models. *Available at SSRN 4484416* .

Buechel S, Hahn U (2017) Emobank: Studying the impact of annotation perspective and representation format on dimensional emotion analysis. *Proceedings of the 15th Conference of the European Chapter of the Association for Computational Linguistics: Volume 2, Short Papers*, 578–585.

Cheng M, Ofek E, Yoganarasimhan H (2025) Balancing engagement and polarization: Multi-objective alignment of news content using llms. *arXiv preprint arXiv:2504.13444* .

Goli A, Singh A (2024) Frontiers: Can large language models capture human preferences? *Marketing Science* 43(4):709–722.

Gui G, Toubia O (2023) The challenge of using LLMs to simulate human behavior: A causal inference perspective. *arXiv preprint arXiv:2312.15524* .

Han Z, Gao C, Liu J, Zhang J, Zhang SQ (2024) Parameter-efficient fine-tuning for large models: A comprehensive survey. *arXiv preprint arXiv:2403.14608* .

Hernandez D, Kaplan J, Henighan T, McCandlish S (2021) Scaling laws for transfer. *arXiv preprint arXiv:2102.01293* .

Hoffmann J, Borgeaud S, Mensch A, Buchatskaya E, Cai T, Rutherford E, Casas DdL, Hendricks LA, Welbl J, Clark A, et al. (2022) Training compute-optimal large language models. *arXiv preprint arXiv:2203.15556* .

Hu EJ, Shen Y, Wallis P, Allen-Zhu Z, Li Y, Wang S, Wang L, Chen W, et al. (2022) Lora: Low-rank adaptation of large language models. *ICLR* 1(2):3.

Ji W, Lei L, Zrnic T (2025) Predictions as surrogates: Revisiting surrogate outcomes in the age of ai. *arXiv preprint arXiv:2501.09731* .

Kaplan J, McCandlish S, Henighan T, Brown TB, Chess B, Child R, Gray S, Radford A, Wu J, Amodei D (2020) Scaling laws for neural language models. *arXiv preprint arXiv:2001.08361* .

Krsteski S, Russo G, Chang S, West R, Gligorić K (2025) Valid survey simulations with limited human data: The roles of prompting, fine-tuning, and rectification. *arXiv preprint arXiv:2510.11408* .

Li A, Chen H, Namkoong H, Peng T (2025) Llm generated persona is a promise with a catch. *arXiv preprint arXiv:2503.16527* .

Li P, Castelo N, Katona Z, Sarvary M (2024) Frontiers: Determining the validity of large language models for automated perceptual analysis. *Marketing Science* .

Liu H, Tang Y, Zhang Z, Zheng Z, Zhu T (2024) Large language model assisted experiment design with generative human-behavior agents. *2024 Winter Simulation Conference (WSC)*, 2751–2762 (IEEE).

Motoki F, Pinho Neto V, Rodrigues V (2024) More human than human: measuring chatgpt political bias. *Public Choice* 198(1):3–23.

Ouyang L, Wu J, Jiang X, Almeida D, Wainwright C, Mishkin P, Zhang C, Agarwal S, Slama K, Ray A, et al. (2022) Training language models to follow instructions with human feedback. *Advances in neural information processing systems* 35:27730–27744.

Peng T, Gui G, Merlau DJ, Fan GJ, Sliman MB, Brucks M, Johnson EJ, Morwitz V, Althenayyan A, Bellezza S, et al. (2025) A mega-study of digital twins reveals strengths, weaknesses and opportunities for further improvement. *arXiv preprint arXiv:2509.19088* .

Pezeshkpour P, Hruschka E (2024) Large language models sensitivity to the order of options in multiple-choice questions. *Findings of the Association for Computational Linguistics: NAACL 2024*, 2006–2017.

Rafailov R, Sharma A, Mitchell E, Manning CD, Ermon S, Finn C (2023) Direct preference optimization: Your language model is secretly a reward model. *Advances in neural information processing systems* 36:53728–53741.

Russell JA, Mehrabian A (1977) Evidence for a three-factor theory of emotions. *Journal of Research in Personality* 11(3):273–294.

Toubia O, Gui GZ, Peng T, Merlau DJ, Li A, Chen H (2025) Database report: Twin-2k-500: A data set for building digital twins of over 2,000 people based on their answers to over 500 questions. *Marketing Science* .

Vafa K, Athey S, Blei DM (2025) Estimating wage disparities using foundation models. *Proceedings of the National Academy of Sciences* 122(22):e2427298122.

Wang M, Zhang DJ, Zhang H (2024) Large language models for market research: A data-augmentation approach. *arXiv preprint arXiv:2412.19363* .

Wei J, Wang X, Schuurmans D, Bosma M, Xia F, Chi E, Le QV, Zhou D, et al. (2022) Chain-of-thought prompting elicits reasoning in large language models. *Advances in neural information processing systems* 35:24824–24837.

Ye Z, Yoganarasimhan H, Zheng Y (2025) LOLA: LLM-assisted online learning algorithm for content experiments. *Marketing Science* .

Zhang B, Liu Z, Cherry C, Firat O (2024) When scaling meets llm finetuning: The effect of data, model and finetuning method. *arXiv preprint arXiv:2402.17193* .

Ziems C, Held W, Shaikh O, Chen J, Zhang Z, Yang D (2024) Can large language models transform computational social science? *Computational Linguistics* 50(1):237–291.

Online Appendix

EC.1. Missing Proofs

EC.1.1. Proof of Theorem 1

Proof of Theorem 1. We consider the optimization problem as in (3). Denote

$$V(s) = \frac{as^{-\alpha} + b}{n - s}.$$

We then find the first order derivative,

$$\begin{aligned} V'(s) &= \frac{-\alpha as^{-\alpha-1}(n-s) + (as^{-\alpha} + b)}{(n-s)^2} \\ &= \frac{-\alpha ans^{-\alpha-1} + (\alpha+1)as^{-\alpha} + b}{(n-s)^2}. \end{aligned}$$

Setting $V'(s) = 0$, we have

$$\alpha ans^{-\alpha-1} - (\alpha+1)as^{-\alpha} - b = 0. \quad (\text{EC.1})$$

Let $h(s) = \alpha ans^{-\alpha-1} - (\alpha+1)as^{-\alpha}$. Then we know $h'(s) = -\alpha(\alpha+1)\left(\frac{n}{s} - 1\right)as^{-\alpha-1} < 0$. This means that the left-hand side of (EC.1) is monotone decreasing. Note that, when $s \rightarrow 0^+$, the left-hand side of (EC.1) can be expressed as $as^{-\alpha}\left(\frac{\alpha n}{s} - \alpha - 1\right) - b \rightarrow +\infty$. When $s = n$, the left-hand side of (EC.1) can be expressed as $-an^{-\alpha} - b < 0$. So there exists a unique solution s^* between 0 and n that solves equation (EC.1).

□